IOSR Journal of VLSI and Signal Processing (IOSR-JVSP)
Volume 16, Issue 1 (Mar. - Apr. 2026), pp. 01-08
e-ISSN: 2319-4200, p-ISSN: 2319-4197
www.iosrjournals.org

A Staggered PRF MTI Ground Radar Simulator For Space Time Processing In Multi-Target And Jamming Environments

Venkata Krishna Rao Maddela
Independent Researcher, IEEE Senior Member
(Previously) Dept Of CSE (Data Science) / Dept Of Electronics & Communication Engineering,
Institute Of Aeronautical Engineering, Hyderabad, India

Abstract
The traditional moving target indicator (MTI) radars perform range-doppler processing using MTI filters or FFT filter bank for ground clutter rejection and identifying and estimating velocities of the moving targets. These radars may use physical antennas with tracking capability or phased array antennas to electronically scan the beam. The radar may also employ Space Time Processing (STP)with an electronically scanned antenna beam to spatially filter out the clutter and to identify the target directions. The stand-alone narrow band DOA techniques are highly matured, space time processing of wideband (e.g., multi frequency) radars, especially the adaptive version of space time adaptive processing (STAP) continues to be an interesting task. The scenario of multiple targets, multiple pulse repetition frequencies (PRFs), diverse clutter types and jamming make the radar receiver processing even more complex. A radar simulator is very useful to test the target detection and estimation algorithms. In this work, a staggered pulse repetition frequency (PRF) radar simulator is proposed. MTI radar scenarios such as multiple targets, multiple clutters and jamming sources are also simulated. The synthetic echo signal data is validated using a basic STP algorithm. The Range-Angle, the Doppler-Angle and the Velocity-Angle maps are produced by spatial time processing. The spatial beam patterns to capture the direction of arrival (DOA) of the targets are plotted and beamwidths are computed. Results confirmed the accuracy and usefulness of the simulated data.

Keywords - *Space Time Processing, Staggered PRF, MTI Radar, Pulse-doppler processing.*

Date of Submission: 03-03-2026 Date of Acceptance: 13-03-2026

I. Introduction

An MTI radar transmits RF waves to illuminate the targets and receives echoes from targets. However, clutter echo from ground and high-power interference signal from jammer sources are also received along with the low-power target echo signals. The traditional moving target indicator (MTI) radars perform range-doppler processing using MTI filters or doppler filter bank to detect moving targets by rejecting clutter from ground [1,2]. These radars use physical antennas with angle tracking capability which provide separate bearing information. Parisa Parhizgar et. al. [3] implemented a range-gated Doppler filterbank on a 16-bit fixed-point DSP processor. The paper also reported the simulation studies on both parametric and non-parametric and spectral estimation techniques for suppressing ground clutter. The proposed technique was a hybrid of a P-order Autoregressive model and N-point FFT technique. However, authors did not specify explicitly the values of P and N. Mohammad A. R., et. al. [4] carried out yet another review of staggered MTI radar theory. Riabukha, V.P., Semeniaka, A.V., et. al. [5] performed seminatural experiments on an adaptive MTI system based on adaptive lattice filter (ALF) using recordings of real clutter and interference parameters extracted from the input signals. It was shown that the adaptive ALF-based MTI system outperformed the traditional non-adaptive MTI system. In place of physical antennas, phased array antennas are also used to electronically scan the antennas beam [6]. Jamming signals can be heavily suppressed by forming nulls in the direction of jammers. Similarly narrow beam(s) can be formed to illuminate only the desired targets and mitigate the clutter returns and other interference signals from other directions. These techniques are collectively known as beamforming or spatial filtering [7, 8]. The combination of spatially filtering the radiation dynamically in time within the antenna subsystem and passing the spatially filtered signals to the receiver for further processing is popularly known as spatial time adaptive processing (STAP) [9, 10, 11]. Modern radars are designed to have STP capability and lot of research and development has been reported in the literature on STP and STAP techniques for more than a decade [12, 13]. Yao Gu., et. al. [14] used a 5-layer 2-D convolutional neural network trained with a low-

resolution angle-doppler spectrum of clutter-plus-target estimated by a few samples. Results show that the targets were detected with a higher detection probability even in the non-homogeneous clutter environments and low signal-to-clutter ratio. Jingwei. X, Shengqi, Zhu. and Guisheng, Liao. [15] proposed spacetime-range adaptive processing based on subspace projection to mitigate the clutter and jamming. A frequency diverse array (FDA) was used for transmission to control the degrees of freedom in both range and angle. domains. Simulation results show that the target was well discriminated against the clutter and jamming as seen in the joint range-angle-doppler maps. C. Cao, et. al, [16] proposed a target detection method exploiting the different motion variations of radar moving target and sea clutter in the range-doppler spectrum sequence. The method used a low-rank representation to separate the target from clutter. The sea clutter data were collected by an X-band radar flying at an altitude of 3 km. The experimental results show that the figure of merit of the proposed method outperformed the constant false alarm rate (CFAR) and principal component pursuit (PCP) methods even in case of slow or weak targets. The design and testing of STP receivers is complex, computationally intensive and needs more hardware resources, and hence costly. A simulator which can generate representative target echoes, clutter and interference signals from selected directions is very useful in testing STP receivers and their submodules.

In the present study the echo signals of a staggered pulse repetition frequency (SPRF) MTI radar engaged in multi-target environment and simultaneously under jamming are simulated. The simulator output can be injected into the baseband module i.e. after the RF/IF stage through proper hardware interface, and functionally of the STP algorithms and STP receivers can be tested using joint space-range-doppler processing. The echo signals generated by an MTI ground are simulated given the radar and target parameters. The clutter and jammers are also simulated with a given power, spatial extent and direction of arrivals. The simulated echo data is stored in a 5-dimensional data cube, which is more suitable for STP receiver processing. A preliminary STP is carried out to verify whether the echoes are properly generated with the stipulated parameters. Results are presented as plots and images. The results are very satisfactory except for the errors due to spatial and temporal quantization used in processing the echo data.

The paper is structured as follows. In section II the mathematical framework related to echo signal generation of the radar under study is discussed. In Section IV the details of simulations and simulations environment are discussed. The tests to validate the data generated and the results are also presented. In Section V conclusions are drawn and scope of future work is projected.

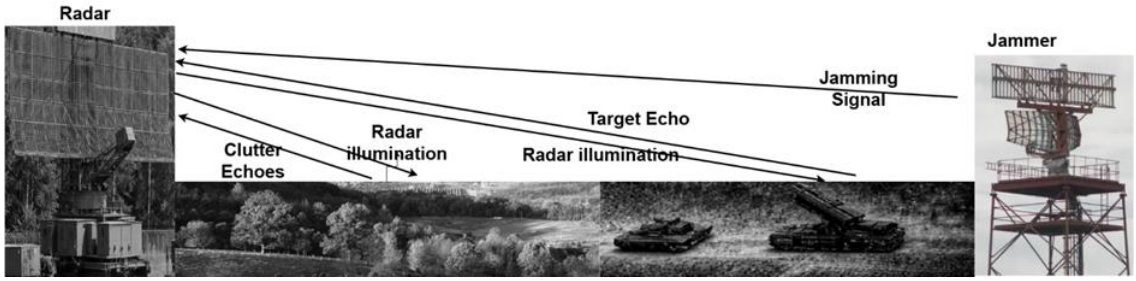

Figure1. A Scenario of a 2-D Ground Scanning MTI Radar

II. Methodology

The echo signal at the input of a radar receiver is the summation of target returns, clutter returns, interference sources (e.g., jammers) and the receiver noise. The received echo signal of an airborne staggered PRF MTI radar for p-th transmitted PRF pulse is given by

$$x_p(m,n,r) = x_{pt}(m,n,r) + x_{pc}(m,n,r) + x_{pj}(m,n,r) + \ x_{pn}(m,n,r) \ldots\ldots\ldots\ldots\ldots\ldots\ldots\ldots\ldots (1)$$

where:

$r = 1, 2, \ldots, R$ is the range bin index

$m = 1, 2, \ldots, M$ is the array element index

$n = 1, 2, \ldots, N$ is the PRF pulse (doppler) index

$p = 1, 2, \ldots, P$ is the PRF index

$x_{pt}(m,n,r)$ are the echo returns from the target(s) for p-th PRF transmission.

$x_{pc}(m,n,r)$ are the echo returns from the clutter(s) for p-th PRF transmission.

$x_{pj}(m,n,r)$ are the interference signals from the jammer(s) for p-th PRF transmission.

$x_{pn}(m,n,r)$ is the system's additive white gaussian noise (AWGN)

The individual components of the eq. (1) are given below [10]

$$x_{pt}(m,n,r) = \sum_{i=1}^{N_T} A_{Ti} S_T(\theta_{si}, \phi_{di}) \delta(r - r_i) \ldots\ldots\ldots\ldots\ldots\ldots\ldots\ldots\ldots\ldots\ldots\ldots\ldots\ldots (2)$$

where:
N_T is the number of targets
$r_i; i = 1, 2, \dots, N_T$ are the target ranges
$A_{Ti}; i = 1, 2, \dots, N_T$ are the target echo amplitudes
$\theta_{si}; i = 1, 2, \dots, N_T$ are the target spatial steering vectors
$\phi_{di}; i = 1, 2, \dots, N_T$ are the target doppler (temporal) steering vectors
$S_T(\theta_{si}, \phi_{di}); i = 1, 2, \dots, N_T$ are the target spatial- temporal steering vectors.

$$x_{pc}(m, n, r) = \sum_{j=1}^{N_C} A_{Cj} S_{Cj}(\theta_{sj}, \phi_{dj}) \delta(r - r_j) \quad \dots\dots\dots\dots\dots\dots\dots\dots\dots\dots\dots\dots\dots\dots\dots (3)$$

where:
N_C is the number of clutters
$r_j; j = 1, 2, \dots, N_J$ are the clutter ranges
$A_{Cj}; j = 1, 2, \dots, N_J$ are the clutter echo amplitudes
$\theta_{sj}; j = 1, 2, \dots, N_J$ are the clutter spatial steering vectors
$\theta_{dj}; j = 1, 2, \dots, N_J$ are the clutter temporal steering vectors
$S_C(\theta_{sj}, \phi_{dj}); i = 1, 2, \dots, N_J$ are the clutter spatial- temporal steering vectors.

$$x_{pj}(m, n, r) = \sum_{k=1}^{N_J} A_{Jk} S_J(\theta_{sk}, \phi_{dk})\, \delta(r - r_k) \quad \dots\dots\dots\dots\dots\dots\dots\dots\dots\dots\dots\dots\dots\dots\dots (4)$$

where:
N_J is the number of jammers
$r_k; k = 1, 2, \dots, N_J$ are the jammer ranges
$A_{Jk}; k = 1, 2, \dots, N_J$ are the jammer echo amplitudes
$\theta_{sk}; k = 1, 2, \dots, N_J$ are the jammer spatial steering vectors
$\phi_{dk}; k = 1, 2, \dots, N_J$ are the jammer temporal steering vectors
$S_J(\theta_{sk}, \phi_{dk}); k = 1, 2, \dots, N_J$ are the jammer spatiotemporal steering vectors.

$$x_{pn}(m, n, r) = \sigma_w\, w_p(m, n, r) \quad \dots\dots\dots\dots\dots\dots\dots\dots\dots\dots\dots\dots\dots\dots\dots (5)$$

where:
σ_w is the RMS amplitude of noise
w_p is the noise that adds to the received signal for p-th PRF.
$n = 1, 2, \dots, N$ is the PRF pulse (doppler) index
$p = 1, 2, \dots, P$ is the PRF index
The spatiotemporal steering vector is given as the knocker product of $S(\theta_s)$ and $S(\phi_d)$ and is given by

$$S(\theta_s, \phi_d) = S(\theta_s) \otimes S(\phi_d) \quad \dots\dots\dots\dots\dots\dots\dots\dots\dots\dots\dots\dots\dots\dots\dots (6)$$

where the spatial steering vector $S(\theta_s)$ is given by

$$S(\theta_s) = e^{j2\pi dm \sin\theta_s}; m = 1, 2, \dots, M \quad \dots\dots\dots\dots\dots\dots\dots\dots\dots (7)$$

and the temporal (doppler) steering vector $S(\phi_t)$ is given by

$$S(\phi_d) = e^{j2\pi f_d nT}; n = 1, 2, \dots, N \quad \dots\dots\dots\dots\dots\dots\dots\dots\dots (8)$$

where f_d is the doppler frequency and T is pulse repetition interval i.e., inverse of the pulse repetition frequency (PRF). The subscripts t, c and j are used for steering vectors to represent the target, clutter and jammer respectively. It may be noted that all signals and noise are complex values having both magnitude and phase.

III. Simulations And Results

The MTI radar echo signals are simulated using the radar and array parameters listed in Tables 1, 2 and 3. The PRFs selected for simulations are 15000Hz, 13695Hz and 16305Hz. The latter two PRFs form ratios with the first PRF are 0.9130 and 1.0870 respectively. It may be verified that these PRFs combinedly offer an unambiguous range of around 114.9 km, which is much higher than the unambiguous range individually provided by these PRFs [18]. The number of doppler bins is a design parameter. Here it is taken as 64 for convenience and gives a doppler resolution of 15000/64 = 234.38Hz. If the doppler bins are increased to 512 or 1024, the resolution increases to 19.53Hz or 9.766Hz respectively. Antenna arrays with $M = 16$ and $M = 32$ are used in this work. The related parameters are given in Table 3.

Table1. Radar System Parameters

	PRF: 13.695 kHz	PRF: 15 kHz	PRF: 16.305kHz
Pulse Repetition Interval (μs)	73.02	66.67	61.33
Operating Frequency (GHz)	10	10	10
Operating Wavelength (cm)	30	30	30

Pulse width (μs)	0.1		0.1		0.1	
Range Resolution (m)	15		15		15	
No. of Range bins	730		666		613	
Unambiguous Range Limits (m)	15	10950	15	9990	9195	
Unambiguous Doppler Limits (Hz)	-6847.5	6847.5	-7500	7500	-8152.5	8152.5
Unambiguous Velocity Limits (m/s)	-102.7	102.7	-112.5	112.5	-122.3	122.3
No. of Doppler bins	64		64		64	
Doppler Resolution (Hz)	213.98		234.38		254.8	

Table 2. Antenna Array Parameters

	Configuration-1	Configuration-2
Geometry	Uniform Linear Array	Uniform Linear Array
No of Elements, M	16	32
Directive Gain, G (Approximate)	16	32
Operating Wavelength, λ (cm)	30	30
Element Spacing in λs	$\lambda/2$	$\lambda/2$
Physical Aperture Size in λs i.e., $(M-1)\lambda/2$	7.5 λ	15.5 λ
Effective Aperture [17] i.e., $\approx \frac{M\lambda^2}{4\pi}$	$1.27\lambda^2$	$2.54\lambda^2$
Half-power beamwidth in radians [17] i.e., $\approx \frac{0.886\lambda}{Nd}$	6.34^o	3.17^o

The algorithm used for simulation is given step-by-step as follows.

1. Read the radar system parameters and array parameters from Tables 1 and 2 respectively.
2. Read the target, clutter, interference (jammer) and noise parameters from Table 3.
3. Initiate the PRF loop.
4. Compute the maximum unambiguous range, maximum unambiguous doppler limits and corresponding range bins and doppler bins for the current PRF.
5. Create a 5-dimensional Data cube: $DC\{i, j, k\ l, m\}$; i as the array element index, j as the number of snapshots (here number PRF pulses), k as the range bin index, l as the PRF index. Initialize the cube with all zeros.
6. Read the target information; compute the spatial, the temporal and the spatial-temporal steering vectors using eq(6), (7) and (8) and then compute the snapshot matrix of first target using eq(2).
7. Accumulate the snapshot matrix into Data cube at corresponding range cell of first target.
8. Repeat steps 6 & 7 for all targets.
9. Read the clutter information; compute the spatial, the temporal and the spatial-temporal steering vectors and then compute the snapshot matrix of first clutter cell using eq (3).
10. Accumulate the snapshot matrix into Data cube at corresponding range cell of first clutter cell.
11. Repeat steps 9 & 10 for all clutter cells.
12. Read the jammer information; compute the spatial and the temporal steering vectors and then accurate the snapshot matrix of first jammer using eq (4).
13. Accumulate the snapshot matrix into Data cube at corresponding range cell of first jammer.
14. Repeat steps 12 & 13 for all jammers.
15. Check if any PRF is left over. If yes, go to next PRF and repeat the steps 4 – 14. Else go to next step.
16. Store the Data cube into permanent memory for later processing together with Radar, Array and Target scenario parameters.
17. Stop.

The algorithm is implemented using basic Matlab instructions without using any toolboxes. The simulations are carried out for three PRFs as stated in Table 1. The data is stored in a *Datacube* structure one for each PRF as shown in Figure 2.

Table 3. Radar Scenario Parameters (used for simulations)

Parameter (units)	Value
No of Targets	**3**
Target Ranges (m)	1500, 9000, 3900
Target Velocities (m/s)	50, 30, -60
Target Dopplers (Hz)	3333, 4000, 3333
Target Azimuth DOAs (deg)	40, 70, 30, -60
Clutter Segment-1	**10**
Clutter Ranges (m)	6360 ± 200 (Random)
Clutter Velocities (m/s)	0, 0, 0, 0
Clutter Dopplers (Hz)	0, 0, 0, 0
Clutter Azimuth DOAs (deg)	-23 ± 10
Clutter Segment-2	**20**
Clutter Ranges (m)	5910 (Linear, Random)

Clutter Velocities (m/s)	0
Clutter Dopplers (Hz)	0
Clutter Azimuth DOAs (deg)	27 ± 20
No of Jammers	**1**
Jammer Range	5250
Jammer Velocity (m/s)	-45
Jammer Doppler (Hz)	-3000
Jammer Azimuth DOA (deg)	70
System Noise (AWGN)	$\boldsymbol{N(0, \sigma_w^2)}$
Noise Power (σ_w^2)	1.0

In this study the target/clutter/jammer ranges and velocities are selected within the unambiguous limits. The results are shown only for one PRF i.e., 15kHz. However, the simulator is more general and can take any ranges and velocities beyond the unambiguous limits also. In such case disambiguation of range or velocity or both is needed in the receiver processing.

To validate the simulated data a basic STP algorithm [19] is implemented using basic Matlab. The Range-Angle (RA) map, The Doppler-Angle (DA) map and the Velocity-Angle (VA) map are shown in Figures 5, 6 and 7 respectively. The target, clutter and jammer amplitudes are respectively determined by the signal-to-noise ratio (SNR), clutter power-to- noise ratio (CNR), and jammer power-to-noise ratio (JNR). In figure 5, 6 and 7, a target SNR of 10dB, a CNR of 10dB and a JNR of 40dB are used. There are two clutter segments. First segment is uniformly distributed around the range of 6360 meter with a maximum spread of 200 meters and is at the mean angle of 27°. The second segment is a random linear cluster centered at the range of 5910 meters and at the mean angle of -23°. There is one jammer source at the range of 4000 meters and at an angle of 27°, and is moving with a velocity of -45 m/s. A negative velocity means the jammer is receding away from the radar, and positive velocities mean the jammer is approaching. All SNRs are computed using unity noise power. All figures are self-explanatory with the simulation parameters printed in the title/ labels/ text. Each target appears as a black pixel and is labelled blue. The jammer source is labelled red. Clutters are label magenta.

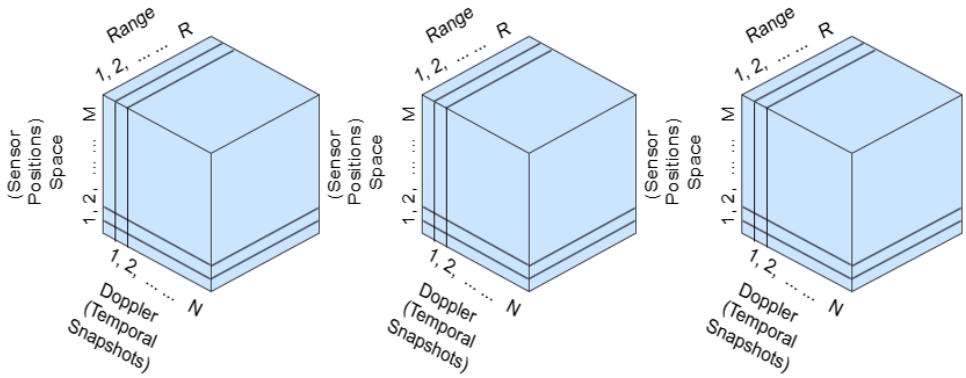

(a). PRF-1 (b). PRF-2 (c). PRF-3

Figure 2. *Datacubes* for echo signal storage

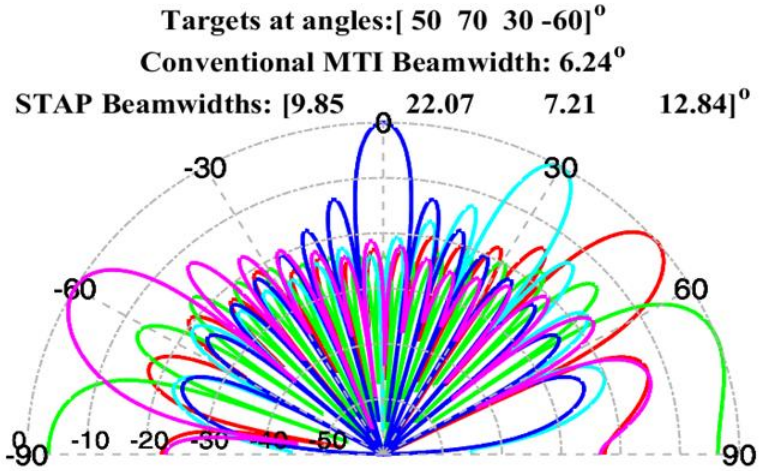

Figure 3. Spatial beams formed by Conventional MTI and STP beams & beamwidths for $M = 16$.

The targets and jammer appear as points in RA map of figure 5, as they are point sources. However, in DA map they appear blurred along azimuth angle due to the scanning of antenna array beam. During scanning the antenna beam convolves with the reflectivity function of a point target. The amount of blurring is determined by the 3-dB beamwidth of the antenna radiation pattern. There is no blurring along range direction as there is no scanning in the radial direction. During scanning the beam moves away from the broadside zero angle, the beam broadens and hence the blurring depends on DOA of the target/ jammer/ clutter bin. It can be clearly seen that the target-3 underwent the least blurring while the jammer (source-2 labelled red) underwent the maximum blurring. The measured beamwidths as determined by the STAP algorithm are printed in the title of the figures 6 and 7, and can be compared with the theoretical values given in Table 3. The discrepancy between the measured and theoretical values are attributed to the azimuth resolution used in the simulation. Here the azimuth angle range of $[-90^o, 90^o]$ is quantized into 180 sectors, giving an angle resolution of 1^o. This quantization error will creep into all calculations based on the DOA angle and directly affects the accuracy in beamwidth measurement and steering vector calculations during data generation and STP processing. As there is no relative motion between radar platform and clutter segments, the two clutter segments are seen at zeroth range bin and extending in azimuth.

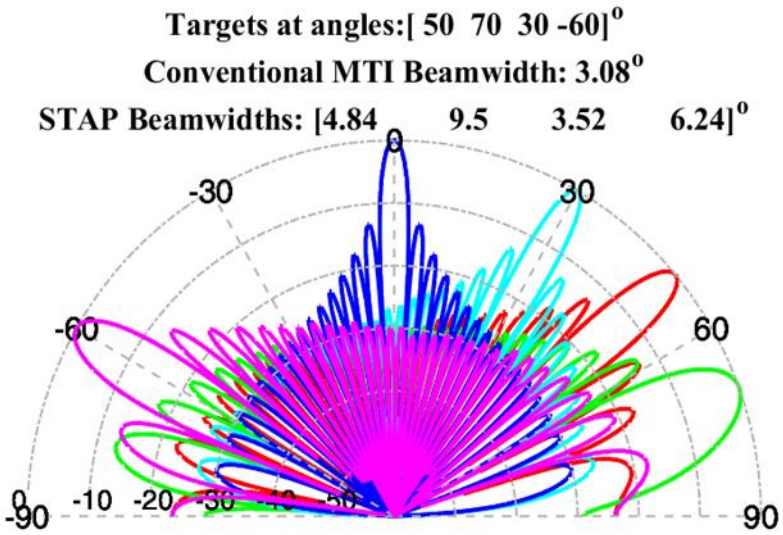

Figure 4. Spatial beams formed by Conventional MTI and STP beams & beamwidths for $M = 32$. The beam at boresight angle (0^o) corresponds to the conventional uniform array (ULA) without beam steering.

The DA and VA maps for SNR of -10dB are shown in Figures 8 and 9. The system noise can be clearly seen in all cells where there is no target or jammer or clutter.

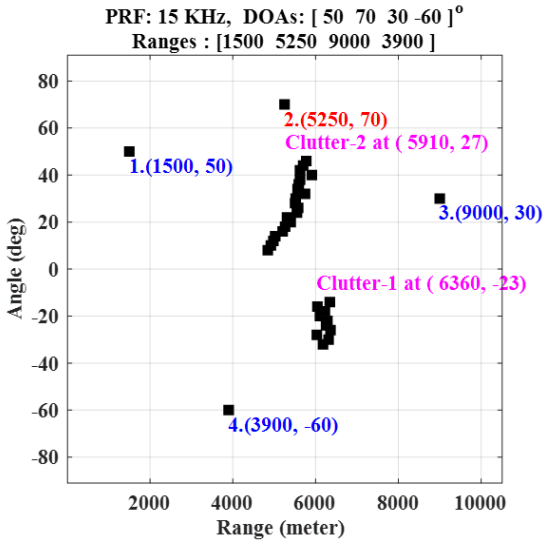

Figure 5. Range-Angle Map at SNRs of 10dB

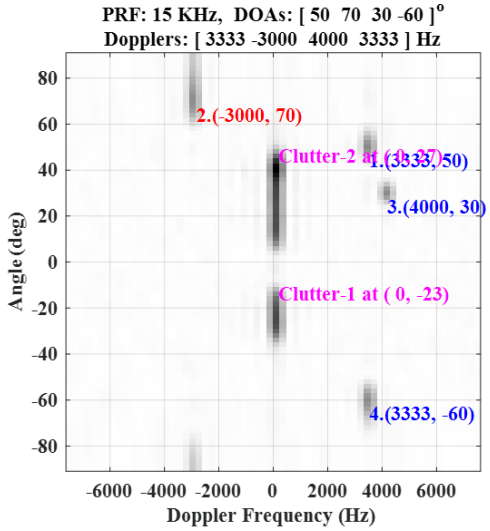

Figure 6. Doppler-Angle Map at SNRs of 10dB

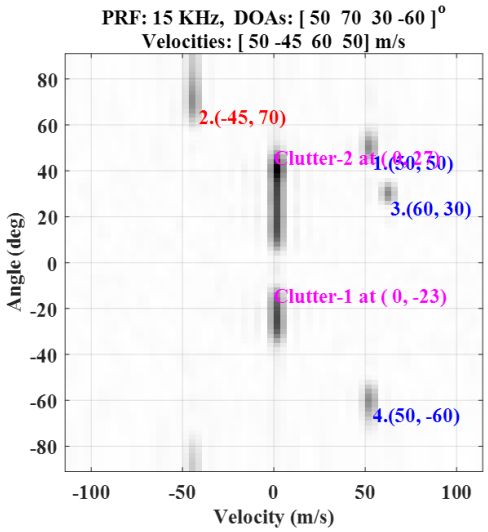

Figure 7. Velocity-Angle Map at SNRs of 10dB

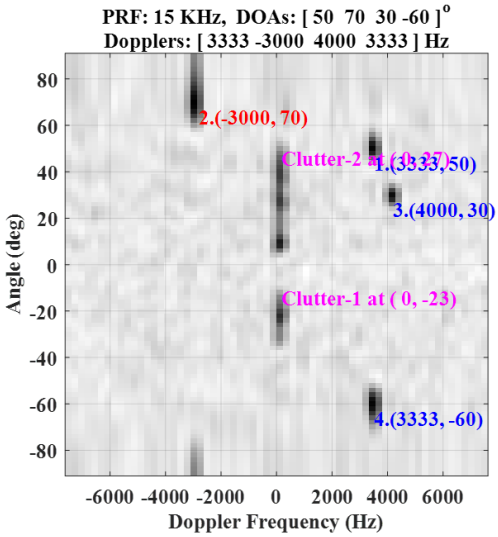

Figure 8. Doppler-Angle Map at SNRs of -10dB

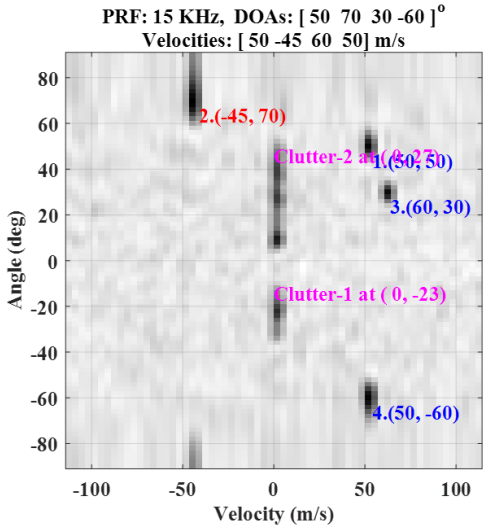

Figure 9. Velocity-Angle Map at SNRs of -10dB

IV. Conclusions And Future Work

A software radar simulator is presented for testing Staggered PRF MTI/ Pulse Doppler radar systems. The generated data is stored as *Datacube*. The data accuracy and usability are tested using a basic STP algorithm. The results are shown as Range-Angle, Range-Doppler and Range-Velocity maps. The targets and other sources of scattering are clearly seen in the Range-Angle map. The velocity of both approaching and receding targets is visualized clearly in both the Range-Doppler and the Range-Velocity maps. The target directions both on the left side and right side of the bore-sight axis are correctly determined. The limitations of this work include the use of point targets, stationary clutter and jammers, narrowband jammers, AWG noise and only azimuth plane.

Future work can consider extended targets, moving clutter and jammers, non-homogeneous clutter, wideband jammers, non-gaussian and correlated noise, and can include elevation also.

References

[1] Merrill I. Skolnik, Introduction To Radar Systems, 2nd Edition, 1981, Mcgraw-Hill.
[2] Fred E Nathanson, Radar Design Principles, 2nd Edition, 1991, Mcgraw-Hill.
[3] Parhizgar, Parisa & Parhizgar, Parsa & Parhizgar, Naser & Dehghani, Zahra. Implementation Of Digital Signal Processor For Pulse Doppler Radar. Computer Networks And Communications. 2023; 1(2): 309-324 Https://Doi.Org/10.37256/Cnc.12202336 89
[4] Mohammad A. Rahaman, Et. Al., A Study On Digital MTI Processors & Frequency Pulse, International Journal Of Innovative Science And Research Technology, October 2025, 10(10): 1820-1837. Https://Www.Ijisrt.Com/A-Study-On-Digital-Mti-Processors-Frequency-Pulse
[5] Riabukha, V.P., Semeniaka, A.V.,. Et Al. Comparative Experimental Investigations Of Adaptive And Non-Adaptive MTI Systems In Pulse Radars Of Various Applications And Wave Ranges. *Radioelectronics And Communications Systems,* 2022, 65:165–176. Https://Doi.Org/10.3103/S073527272204001X
[6] R. C. Hansen, Phased Array Antennas, 2nd Edition, 2009, John Wiley & Sons, Inc.
[7] B. D. Van Veen And K. M. Buckley, "Beamforming: A Versatile Approach To Spatial Filtering," *IEEE ASSP Magazine*, April 1988, 5(2): 4-24, Https://Doi.Org/10.1109/53.665
[8] Robert J. Mailloux, Phased Array Antenna Handbook, 2nd Edition, Artech House, Inc., 2005, Norwood, MA.
[9] Christian, W., Christina, B., Timo, G., Millimeter Wave Radar: Hardware And Signal Processing, Springer, 2025.
[10] Chen, Joe & Yao, Kung & Hudson, Ralph., Source Localization And Beamforming, Signal Processing Magazine, IEEE, 2002, 19: 30-39, Https://Doi.Org/10.1109/79.985676
[11] Robert A. Monzingo, Randy L. Haupt And Thomas W. Miller, Introduction To Adaptive Arrays, 2nd Edition, 2011, Scitech, Raleigh.
[12] Al-Sadoon, Et. Al., (2020). A New Beamforming Approach Using 60 Ghz Antenna Arrays For Multi-Beams 5G Applications. Electronics 2022, 11(11): 1-22. Https://Doi.Org/10.3390/Electronics11111739
[13] Omolaye, P, & Adeleye, S, Et. Al. AI-Assisted Adaptive Beamforming Antennas For Dynamic Spectrum Access. American Journal Of Networks And Communications. 2026, 15(1): 1–9. Https://Doi.Org/10.11648/J.Ajnc.20261501.11
[14] Yao Gu. Et. Al., End-To-End Moving Target Indication For Airborne Radar Using Deep Learning, Remote Sensing, MDTI, 2022 Https://Www.Mdpi.Com/2072-4292/14/21/5354
[15] Jingwei Xu, Shengqi Zhu, And Guisheng Liao, Space-Time-Range Adaptive Processing For Airborne Radar Systems, IEEE Sensors Journal, March 2015, 15(3):1602-1610. Https://Doi.Org/10.1109/JSEN.2014.2364594
[16] C. Cao, Et. Al., Clutter Suppression And Target Tracking By The Low-Rank Representation For Airborne Maritime Surveillance Radar," *IEEE Access*, 2020, 8: 160774-160789. Https://Doi.Org/10.1109/ACCESS.2020.3021124
[17] John D. Kraus, Electromagnetics, International Student Edition, 3rd Edition, Mcgraw-Hill, 1984.
[18] Tang, Lei., He Core Progress Of Staggered PRF Modulation Technique In MTI Radar. 2023: 1-6 . Https://Doi.Org/10.36227/Techrxiv.22301098
[19] Guerci, J. R. *Space-Time Adaptive Processing For Radar*. Artech House Radar Library. Boston: Artech House, 2003.